

# Online Trajectory Optimization for Persistent Monitoring Problems in Partitioned Environments

Jonas Hall<sup>1</sup>, Christos G. Cassandras<sup>1,2</sup>, Sean B. Andersson<sup>1,3</sup>

**Abstract**—We consider the problem of using an autonomous agent to persistently monitor a collection of dynamic targets distributed in an environment. We generalize existing work by allowing the agent’s dynamics to vary throughout the environment, leading to a hybrid dynamical system. This introduces an additional layer of complexity towards the planning portion of the problem: we must not only identify in which order to visit the points of interest, but also in which order to traverse the regions. We design an offline high-level sequence planner together with an online trajectory optimizer realizing the computed visiting sequence. We provide numerical experiments to illustrate the performance of our approach.

## I. INTRODUCTION

Persistent Monitoring (PM) describes a broad class of problems in which an agent moves through an environment to collect information about specific targets over time. It is applicable across a wide range of applications, such as ocean monitoring [1], forest fire surveillance [2], tracking of individual biological macromolecules [3], and data harvesting [4]. As a specific motivating application, consider a disaster scenario. An efficient response to a catastrophic event such as an earthquake, hurricane, or tsunami requires the persistent and simultaneous state estimation of many locations in order to make time-sensitive resource distribution decisions. The affected area may consist of various types of terrain, each having its own characteristics. For instance, some parts may be urban and thus contain obstacles, others may be coastal regions with the presence of strong winds. In this paper, we propose an online trajectory optimization scheme to minimize the average estimation error of the site states for piecewise continuous agent dynamics. These hybrid dynamics have the capability of capturing the various terrains the agent must move through; in turn, this requires the extension of standard trajectory optimizers for PM in order to exploit the local structures.

In this paper, we assume that there are multiple sites to be monitored, each of which is located in a different region. We model the *state* of each site with a stochastic Linear Time-Invariant (LTI) system and assume the agent has the ability to interact with each site in its

vicinity through noisy measurements of this state. To obtain good estimates of the state of site, the agent must navigate to the site and remain nearby to collect measurements over time. However, since the agent is tasked with monitoring all the sites, it cannot spend too much time at each individual site since its knowledge of other sites not being monitored decays. Thus, we want to optimize both the time spent at each location and the sequence of site visits.

The optimization of the visiting sequence is often approached by abstracting the problem to a graph structure and using Traveling Salesperson Problem (TSP) inspired solutions [5] in an offline preparation phase. The generation of such a graph requires the estimation of travel times between sites, which is itself a challenging problem in our setting of hybrid agent dynamics. One conceivable approach to tackle this problem is the utilization of nonsmooth optimal control solvers [6], [7]. However, since they are numerical solvers, they are prone to getting stuck at local minima. Furthermore, they cannot exploit any structure that is specific to each terrain. Since the visiting sequence can be found offline, we do not require solutions in real-time and introduce an algorithm inspired by Rapidly-exploring Random Tree (RRT\*) [8]. The proposed algorithm makes the assumption that regional path planners exist for each terrain type, and then generates a tree of how to reach a site by sampling nodes on the boundaries of the region partitioning. The usage of RRT\* is not novel within PM, e.g., the authors in [9] have proposed a rapidly-exploring random cycle generation algorithm to tackle the entire trajectory planning problem. The search space of all cycles, however, can become extremely large for PM problems. Here, we only use it for the abstract graph generation to plan an appropriate visiting sequence. After determining a visiting sequence, we complete the trajectory by solving local monitoring Optimal Control Problems (OCPs) for each site visit. Finally, we optimize the monitoring durations in an online bilevel optimization scheme.

The bilevel optimization approach builds upon our prior work in [10]. The present paper differs from that effort in many key aspects, including a more realistic model of target uncertainty (described now in terms of variance of the state estimates), a more complex environment, and a focus on minimizing the average uncertainty rather than the period of the trajectory subject to constraints on the uncertainty reduction in each cycle. The contributions of this paper are as follows:

This work was supported in part by the NSF through ECCS-1931600

<sup>1</sup>Division of Systems Engineering, Boston University, USA

<sup>2</sup>Department of Electrical and Computer Engineering

<sup>3</sup>Division of Mechanical Engineering, Boston University, USA  
{hallj, cgc, sanderss}@bu.edu

- We propose a novel PM formulation by introducing piecewise continuous agent dynamics.
- We introduce the Rapidly-exploring Random Boundary Tree (RRBT\*) algorithm for global path planning in the introduced context.
- We introduce an online optimization scheme to minimize the steady-state average estimation error.

The remainder of this paper is organized as follows. In Sec. II we introduce the problem formulation. Sec. III introduces the RRBT\* algorithm, which lays the basis for computing the interregional trajectory segments. We then generate a TSP solution from the graph generated by successive utilization of the RRBT\* algorithm. Using the computed visiting sequence, we discuss the trajectory decomposition into local control segments in Sec. IV. Sec. IV-C then provides the online bilevel optimization of the global cost function by alternating between updates of the local control segments and the global optimization parameters. The efficacy of the method is demonstrated in Sec. V and we conclude the article in Sec. VI while providing open questions for future work.

## II. PROBLEM FORMULATION

As depicted in Fig. 1, we consider a partitioned environment in which a single agent moves to carry out its PM mission. The partition is defined by the agent's dynamics: these dynamics are smooth within any given region but may change abruptly when moving between regions. Each region is assumed to contain at most one target; each target is associated with a set of states that evolve according to stochastic LTI dynamics. The agent is equipped with a sensor that can take noisy measurements of a target's internal states whenever it is within the respective region. In this section we introduce the necessary notation and formally define our PM problem.

For a vector  $x \in \mathbb{R}^n$  we denote its Euclidean norm by  $\|x\|$ . For a given vector  $x$  and a nonnegative scalar  $\alpha \geq 0$  we denote the set of all vectors  $v \in \mathbb{R}^n$  that satisfy  $\|x - v\| \leq \alpha$  by  $B_\alpha(x)$ . For a set  $S \subset \mathbb{R}^n$  we denote its interior by  $\overset{\circ}{S}$ , its closure by  $\bar{S}$ , and its boundary by  $\partial S = \bar{S} \setminus \overset{\circ}{S}$ . By  $\mathcal{B}(\mathbb{R}^n)$  we denote the set of all subsets of  $\mathbb{R}^n$ . Given two paths  $u_1 : [0, T_1] \rightarrow \mathbb{R}^n$ ,  $u_2 : [0, T_2] \rightarrow \mathbb{R}^n$ , we define their concatenation  $u_1 \circ u_2 : [0, T_1 + T_2] \rightarrow \mathbb{R}^n$  as  $(u_2 \circ u_1)(t) = \alpha(t)u_1(t) + (1 - \alpha(t))u_2(t)$ , where  $\alpha(t) \in \{0, 1\}$  is equal to 1 iff  $t \in [0, T_1]$ .

Let us assume that the compact and connected mission space  $S \subset \mathbb{R}^2$  is partitioned into  $P$  polyhedra,

$$S_i = \{x \in \mathbb{R}^2 \mid g_j^\top x \leq b_j \text{ for } j = 1, 2, \dots, P_i\}, \quad (1)$$

for  $i = 1, 2, \dots, P$ , where  $P_i$  denotes the number of inequalities required to describe the set  $S_i$ . We assume that

$$\overset{\circ}{S}_i \cap \overset{\circ}{S}_j = \emptyset \text{ for } i \neq j \quad \text{and} \quad \bigcup_{i=1}^P S_i = S,$$

i.e., we assume that any two sets in the the partition have disjoint interiors and that the union of all sets provides the entire space. The partitioning is illustrated in Fig. 1.

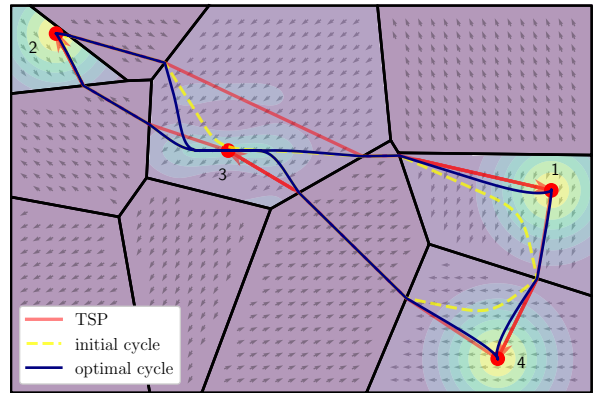


Fig. 1: Illustrating the partitioned mission space based on the piecewise smooth (uncontrolled) agent dynamics together with a comparison of periodic trajectories.

Now, let  $a(t) \in \mathbb{R}^2$  denote the agent's position at time  $t$ . To capture the changing dynamics of the agent, let us define the piecewise smooth vector field

$$f(x) = f_i(x) \text{ if } x \in \overset{\circ}{S}_i, \quad (2)$$

where each  $f_i$  is assumed to be smooth. To extend the dynamics on the switching set  $\mathcal{S}_f = \cup_i \partial S_i$  of the partition, we use the notion of a Filippov set-valued map:

$$\mathcal{F}[f](x) = \bar{co} \left\{ \lim_{x_i \rightarrow x} f(x_i) : x_i \rightarrow x, x_i \notin \mathcal{S}_f \right\}.$$

Note that in the interior of a region  $i$  the set-valued map is the singleton set  $\{f_i(x)\}$  due to the continuity of  $f$ , which shows its consistency with the original vector field (2). Using this notion, we define the agent's dynamics as

$$\dot{a}(t) \in \mathcal{F}[f](a(t)) + u(t),$$

where  $u : [0, \infty) \rightarrow B_1(0)$  is assumed to be an integrable control function. For more details on Filippov differential inclusions, we refer the reader to [11], [12].

We further consider  $M$  targets located at  $p_i \in S_{j_i}$  in some region  $j_i$ . We assume that each region contains at most one target, i.e.,  $j_{i_1} \neq j_{i_2}$  for  $i_1 \neq i_2 \in \mathcal{T} = \{1, 2, \dots, M\}$ . This assumption is not restrictive since we could introduce an additional partition with identical dynamics separating the targets. Each target contains an internal state  $\phi_i(t) \in \mathbb{R}^{m_i}$  following the stochastic LTI dynamics

$$\dot{\phi}_i(t) = A_i \phi_i(t) + \omega_i(t), \quad (3)$$

where  $\omega_i$  is a zero-mean white noise process with covariance  $Q_i \succ 0$ .

The agent is tasked to maintain estimates of all targets' internal states. The only form of interaction between the agent and target  $i$  is described by the sensor's measurement model

$$z_i(a(t), \phi_i(t)) = \gamma_i(a(t))H_i \phi_i(t) + \nu_i(t). \quad (4)$$

Here  $\nu_i$  is a zero mean white noise process with covariance matrix  $R_i$  and  $\gamma_i : \mathbb{R}^2 \rightarrow [0, 1]$  captures the quality

of the measurement depending on the position of the agent. The precise form of this function is not crucial, however, we assume it to (i) be differentiable with respect to the agent position within the region  $S_i$  and (ii) have compact support  $K_i \subseteq S_i$ . We can then write

$$\gamma_i(a(t)) = \begin{cases} 0, & \text{if } a(t) \notin \overset{\circ}{S}_i, \\ \hat{\gamma}_i(a(t)) & \text{if } a(t) \in \overset{\circ}{S}_i, \end{cases} \quad (5)$$

where the  $\hat{\gamma}_i : \mathbb{R}^2 \rightarrow [0, 1]$  is a differentiable function. Fig. 1 illustrates different potential forms of this function, e.g., the region of target 3 has a nonconvex quality mapping; whereas the other regions have Gaussian quality mappings.

From previous results [13] we know that the optimal unbiased estimator of  $\phi_i$  using the measurements from (4) is the Kalman-Bucy filter. The covariance matrix of this estimator is given by

$$\begin{aligned} \dot{\Omega}_i(t) &= A_i \Omega_i(t) + \Omega_i(t) A_i^\top + Q_i - \Omega_i(t) G_i(t) \Omega_i(t) \\ &=: f_{\Omega_i}(t), \end{aligned} \quad (6)$$

where

$$G_i(t) = \gamma_i^2(a(t)) H_i^\top R_i^{-1} H_i.$$

The final ingredient required to formulate the introduced problem as an OCP is the choice of a cost function. Some examples of objectives typical to persistent monitoring applications are the minimization of the (i) maximum revisit time [5]; (ii) worst case estimation error [14], [15]; or (iii) average estimation error [16]. In this paper we choose to minimize the average estimation error. Combining all ingredients allows us to formulate the following OCP.

$$\min_u \lim_{T \rightarrow \infty} \frac{1}{T} \int_0^T \sum_{i=1}^M \text{tr}(\Omega_i(t)) dt \quad (7a)$$

$$\text{s.t.} \quad a(0) = \bar{a}, \quad (7b)$$

$$\Omega(0) = \bar{\Omega}, \quad (7c)$$

$$\dot{a}(t) \in \mathcal{F}[f](a(t)) + u(t), \quad (7d)$$

$$\dot{\Omega}_i(t) = f_{\Omega_i}(t) \text{ for all } i, \quad (7e)$$

$$\|u(t)\| \leq 1, \quad (7f)$$

where  $\bar{a}$ ,  $\bar{\Omega}$  fix the initial states.

**Assumptions.** *Throughout this paper we assume that*

- the pair  $(A_i, H_i)$  is observable for all  $i \in \mathcal{T}$ ; and
- $Q_i$  and  $\Omega_i(0)$  are positive definite for all  $i \in \mathcal{T}$ .

These assumptions ensure that the covariance matrix  $\Omega_i(t)$  is positive definite for all  $t \geq 0$  and that the covariance matrix trajectories eventually become periodic under any periodic control law [17]. It is well known that periodic trajectories have the capability of approximating the optimal cost of average infinite horizon problems arbitrarily well [18], and we thus restrict our attention to periodic control laws. This allows the reformulation of

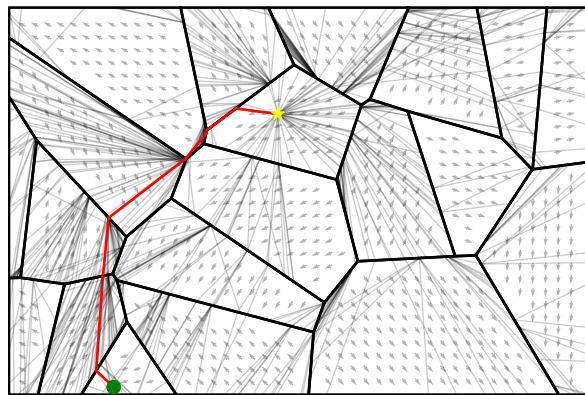


Fig. 2: Illustrating the used global path planner based on an RRBT\* algorithm and we use it to find a global path from the initial node (green circle) to the root node (yellow star).

the infinite horizon OCP (7) to a finite horizon problem by optimizing the steady-state average cost

$$J = \frac{1}{T} \int_0^T \sum_{i=1}^M \text{tr}(\Omega_i(t)) dt, \quad (8)$$

over a cycle of period  $T$ . The following section introduces the offline global planner, which we utilize in order to determine a periodic visiting sequence.

### III. GLOBAL PLANNING

As illustrated by the yellow dashed curve in Fig. 1, an optimal trajectory is comprised of (i) the sequence in which the targets are visited; (ii) the points on the partition set boundaries where the agent changes its mode; (iii) the trajectories connecting the points from (ii) of one target region to the next; and (iv) the local monitoring segments within each target region. Note that since the agent does not sense any of the targets along trajectory segments in (iii), these trajectories must be time-optimal for the overall trajectory to be optimal. Optimizing (i)-(iii) can be done offline; in this section we develop heuristics for this. Sec. IV then introduces the optimization of (iv), which is done online.

The goal of this section is to find a periodic target visiting sequence  $(i_1, i_2, \dots, i_K)$ , where  $K$  is the length of that sequence, together with the time optimal switching segments between the target regions  $i_k$  to  $i_{k+1}$ . We do this by abstracting the mission space to a graph, where each node represents a target and each directed edge denotes the minimum time required to travel from one node to the other. Given such a graph we seek a minimum time cycle that visits all targets, i.e., we want to solve a TSP problem, which is NP-hard in and of itself. Such a path is illustrated by the (directed) red line in Fig. 1. Depending on the number of targets we can use an exact solver or resort to heuristics.

In order to generate the graph introduced above, we must compute the minimum time required to travel between any pair of targets. To do this, we created an

algorithm inspired by RRT\* [8] in order to generate a global search tree capturing minimum-time paths to each target  $i_\ell$  from anywhere in the mission space. The main difference from the formulation in [8] is the presence of the hybrid dynamics. We exploit the partition structure by assuming the existence of a local controller for each region  $i$  with the capability of computing a (time optimal) control law that steers the agent from  $x$  to  $y$  within region  $S_i$ . We denote the time required to do so by

$$\delta_i(x, y) : S_i \times S_i \rightarrow \mathbb{R}_{\geq 0} \cup \{\infty\}. \quad (9)$$

Note that while we assume  $\delta$  to be time optimal, the rest of our approach does not strictly require it; the resulting paths would, of course, be suboptimal. With this abstraction, we can modify the original RRT\* algorithm to produce a search tree on which all nodes, apart from the root node, lie on the boundary sets of the partition. Below we describe the RRBT\* algorithm in more detail. A brief pseudo-code overview is provided in Algorithm 1. In Fig. 2 we illustrate an example of a search tree generated for the root node (yellow) together with a particular path from another node (green).

Given a point  $x$  in the mission space, we initialize the tree of the RRBT\* algorithm by creating a root node at  $x$ , and we initially *activate* all regions which contain the root node. Active regions are all regions that have a representative within the tree; this is a necessary condition that guarantees a newly sampled node from that region can be connected to the tree by using the respective local controller (9). Note that only one region is initially activated if the root lies in the interior of a partition set. Otherwise multiple regions are activated, since each set of the partition is closed (1).

Let us now walk through a main iterate. The sampling phase aims to generate a new node to be included into the tree. We do this by first uniformly sampling a region  $r$  from the active regions. We then uniformly sample a boundary point  $b$  from that region  $r$ , which provides the new node. The neighborhood of a boundary point  $b$ , denoted  $N(b)$ , is defined to be the set of all nodes in the tree that share a region with the sampled boundary point. Note that  $N(b)$  is not empty by design. Given a potential parent  $p \in N(b)$ , we can compute an upper bound for the cost-to-root  $c(b, x)$  by passing through  $p$ , i.e.,  $c(b, x) \leq \delta_r(b, p) + c(p, x)$ . We then connect the newly sampled node to the parent that minimizes this cost-to-root metric. We repeat this procedure for a predefined number of iterations.

We remark here that if all points in the space are reachable from  $x$  then all regions will eventually become active if we sample long enough, and we can then connect each target to any other target, which is how we plan to use this algorithm. To see this, note that each region only has a finite number boundary segments, each of which has a positive length. Thus, the probability of sampling a point from a specific boundary segment has positive probability. If we sample sufficiently often from one region, every boundary segment will eventually have

a representative and all neighbors will become active. Now let  $r_A$  be some active region and  $r_1$  an arbitrary region. Since the regions are given by a partitioning of a connected space, there is a finite sequence of regions  $(r_1, r_2, \dots, r_A)$ , where each  $r_i$  is a neighbor of  $r_{i\pm 1}$ . Since all neighboring regions of  $r_A$  will eventually become active,  $r_{A-1}$  will also become active, and thus also  $r_{A-2}$ , and so forth, until eventually  $r_1$  will become active.

Once we have generated a search tree from a point  $x$ , we can find a global trajectory from any  $y$  that lies in an active region by performing the connection phase of Algorithm 1 with  $b = y$ . We use this mechanism to generate a tree for each target and then compute the target-to-target distance for each combination.

---

#### Algorithm 1: RRBT\* (from root node $x$ )

---

```

1 # initialization phase
2 initialize tree with root at  $x$ 
3 activate all regions containing  $x$ 

4 # main loop
5 while max iter not exceeded do
6   # sample phase
7   sample  $r$  from all active regions
8   sample boundary point  $b$  from  $r$ 

9   # connection phase
10  get neighborhood  $N(b)$ 
11  find parent  $p \in N(b)$  minimizing cost-to-root
12  connect  $b$  to  $p$ 

13  # activation phase
14  activate any new region containing  $b$ 

```

---

## IV. OPTIMIZING THE AVERAGE CYCLE COST

The algorithm in the previous section generates a periodic visiting sequence  $(i_1, i_2, \dots, i_K)$  together with an initial trajectory of some period  $T$ . Using this initialization, we decompose the control law  $u : [0, T] \rightarrow \mathcal{U}$  into its local segments

$$u = (u_{K-1}^s \circ u_{K-1}^m) \circ \dots \circ (u_1^s \circ u_1^m),$$

where  $u_k^s$  describes the  $k$ th switching control law from target region  $i_k$  to  $i_{k+1}$ , which is obtained using the optimal path generated using the RRBT\* algorithm, and  $u_k^m$  describes the  $k$ th monitoring control law. Fig. 3 depicts this decomposition. The next section focuses on the optimization of the monitoring control laws.

### A. The Local Monitoring Control Problem

The boundary conditions of the monitoring segment are given by the start and end points of the next and previous switching segments, respectively. We denote the agent's entry point of the  $k$ th monitoring segment by  $a_k^\varphi \in \partial S_{i_k}$ , the exit point by  $a_k^\psi \in \partial S_{i_k}$ , the associated duration by  $\tau_k \in \mathbb{R}_{\geq 0}$ , and the initial values of the

estimator's covariance matrices by  $\bar{\Omega}$ . We then define the  $k$ th monitoring OCP:

$$M_k^*(\tau_k) = \min_{\tau, u_k^m} \int_0^\tau \sum_{i=1}^M \text{tr}(\Omega_i(t)) dt \quad (10a)$$

$$\text{s.t.} \quad \tau = \tau_k, \quad (10b)$$

$$a(0) = a_k^\varphi, \quad (10c)$$

$$a(\tau_k) = a_k^\psi, \quad (10d)$$

$$\Omega(0) = \bar{\Omega}, \quad (10e)$$

$$\dot{a}(t) = f_{i_k}(x) + u_k^m(t), \quad (10f)$$

$$\|u_k^m(t)\| \leq 1, \quad (10g)$$

$$\dot{\Omega}_i(t) = f_{\Omega_i}(t) \text{ for all } i, \quad (10h)$$

$$a(t) \in S_{i_k}. \quad (10i)$$

Let us remark here that the dynamics (10f) and (10h) are smooth, as long as the resulting trajectory remains within the region  $i_k$  for all  $t \in (0, \tau_k)$ , which is enforced by the linear path constraints (10i). Note that the local monitoring OCP only affects the estimator's covariance matrix corresponding to the current target  $i_k$  since the sensing quality function for all other targets are zero (see (5)). In view of optimizing (10), removing the states of the targets that are not monitored from (10h) and their associated cost terms leads to the same optimizer. However, in view of the decomposition described in the subsection below, they must be included. Whether these terms are included before or after the optimization has no effect. We include the terms here in order to be consistent with the presentation later on.

Fixing the local monitoring durations  $\tau_k$  allows us to solve the OCP in (10). Analytical solutions may exist for some very particular scenarios, but in order to achieve flexibility with respect to  $f_{i_k}$  and the choice of the sensing quality function we solve this OCP using numerical optimization techniques [19]. Crucially, in order for the local monitoring problem (10) to be consistent, we require that the exit point  $a_k^\psi$  is reachable for the agent from the entry point  $a_k^\varphi$  within  $\tau_k$  units of time, i.e., we must ensure

$$\tau_k \geq \delta_{i_k}(a_k^\varphi, a_k^\psi), \quad (11)$$

where we recall that  $\delta_{i_k}(a_k^\varphi, a_k^\psi)$  is the (minimum) time required to travel from  $a_k^\varphi$  to  $a_k^\psi$  in region  $i_k$ . This constraint will be enforced in the bilevel optimization problem (12) described below.

### B. Global Cost Decomposition

The global cost function (8) can be decomposed into the local cost contributions of the monitoring and switching periods (see again Fig. 3 for an illustration of the decomposition). Recall that the cost of the  $k$ th monitoring period is reflected by  $M_k^*(\tau_k)$  in (10). The cost of the switching period between the  $k$ th and  $(k+1)$ st monitoring period is denoted by

$$S_k = \int_{t_k^{\text{sw}}}^{t_k^{\text{sw}} + \Delta_k} \sum_{i=1}^M \text{tr}(\Omega_i(t)) dt,$$

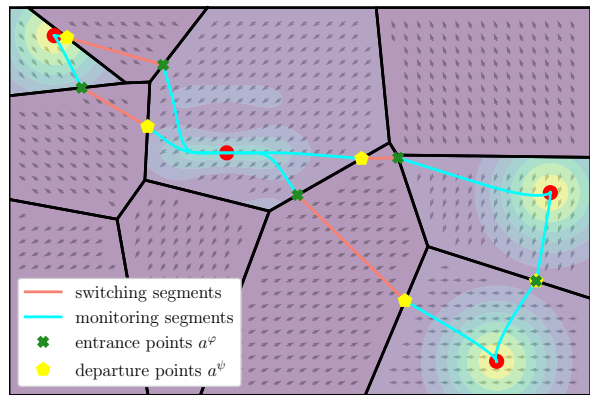


Fig. 3: Illustrating the decomposition into switching and monitoring segments.

where  $\Delta_k = \delta(a_k^\psi, a_{k+1}^\varphi)$  is the (fixed) duration of the  $k$ th switching period and  $t_k^{\text{sw}}$  denotes the starting time of the  $k$ th switching period. Note that the dynamics of the estimator's covariance matrices  $\Omega_i$  are all smooth during the switching segment since no measurements are taken during this interval. Although the agent may traverse multiple regions when transitioning from one target region to the next, none of these traversed regions, by design, contain a target.

With this decomposition, we establish the global bilevel optimization problem

$$\min_{\tau} \frac{1}{T(\tau)} \sum_{k=1}^K (M_k^*(\tau_k) + S_k) \quad (12a)$$

$$\text{s.t.} \quad \tau_k \geq \delta_{i_k}(a_k^\varphi, a_k^\psi) \text{ for } k = 1, \dots, K, \quad (12b)$$

which couples the local segments. The cycle duration in dependence of the monitoring durations is given by

$$T(\tau) = \sum_{k=1}^K (\tau_k + \Delta_k).$$

### C. Optimizing the Monitoring Durations

The gradient of the cost function (12a) with respect to the parameter  $\tau_k$  is given by

$$\frac{dM_k^*(\tau_k)}{d\tau_k} \cdot T(\tau) - \sum_{k=1}^K (M_k^*(\tau_k) + S_k(u_k^s)) \frac{1}{T(\tau)^2}. \quad (13)$$

Note that the gradient  $\frac{dM_k^*}{d\tau_k}$  is the *sensitivity* of the  $k$ th optimal monitoring cost with respect to the parameter  $\tau_k$ . Assuming that strong duality holds in the monitoring OCP (10), we can utilize the shadow price equation [20]

$$\frac{dM_k^*}{d\tau_k} = -\lambda_k,$$

where  $\lambda_k \in \mathbb{R}$  is the dual variable of the equality constraint (10b). This allows us to compute the gradient of the global cost function with respect to the local monitoring durations. We then solve (12) in an alternating fashion, where we fix the monitoring durations and then simulate one (or multiple) cycle(s). Note that simulating

a cycle includes re-solving each monitoring OCP with the updated initial covariance matrices. We utilize the gradient (13) and update the monitoring durations based on a simple projected gradient method with diminishing step size. We compare two optimization methods in the next section:

- (i) Simulating to steady state before updating  $\tau$ .
- (ii) Updating  $\tau$  after every cycle ( $i_1, i_2, \dots, i_K$ ).

The first method is motivated from the fact that the computed gradient (13) describes the steepest ascending direction of the global cycle cost under a given configuration consisting of the monitoring durations and the estimator covariance matrices at the beginning of the cycle. If the cycle is not in steady state, the computed gradient may be inaccurate. On the other hand, the initial configuration, and thus the initial steady-state covariance matrices may be far from the optimal, such that a precise gradient may be unnecessary to obtain. As we decrease the amount of change in the configuration, the cycle will eventually converge to a steady-state cycle, where the gradient will become precise. This motivates the second variant. Although convergence in bilevel optimization problems is difficult to establish, the next section supports that both variants work well in terms of performance.

## V. NUMERICAL RESULTS

We discretize the local monitoring OCP (10b) via a multiple shooting method using the RK4 integrator [19]. We model and solve this via CasADi [21] utilizing the interior-point solver IPOPT [22]. Optimization of the monitoring durations is done using a projected gradient descent with diminishing step size. All simulations were conducted on a hardware featuring an Intel i5 processor running at 1.60GHz with 16GB of RAM. In the following results all regions have randomly generated constant dynamics with norm bounded by one. All targets either have a Gaussian sensing model or a nonconvex sensing model, the exact form of which is omitted here for space reasons. All specific details on problem set up can be found in the provided repository [github.com/hallfjonas/hytoperm](https://github.com/hallfjonas/hytoperm).

We first consider the scenario illustrated in Fig. 1, which contains four targets and ten regions. Fig. 4 compares the two variants (i) and (ii). Note that in this particular scenario, variant (ii) completes its optimization procedure before variant (i) even converges to a steady-state cycle. This is due to the fact that this variant is capable of modifying the monitoring periods more rapidly and as a result the steady-state is reached more quickly. For both variants we see that the objective function is flat near the local optimum, since the cost does not change for the final few iterations while the monitoring durations are still updated. Fig. 5 depicts the controls for the optimal cycle together with the mean estimation errors for variant (i). The results show that throughout the cycle the control constraints  $\|u(t)\| \leq 1$

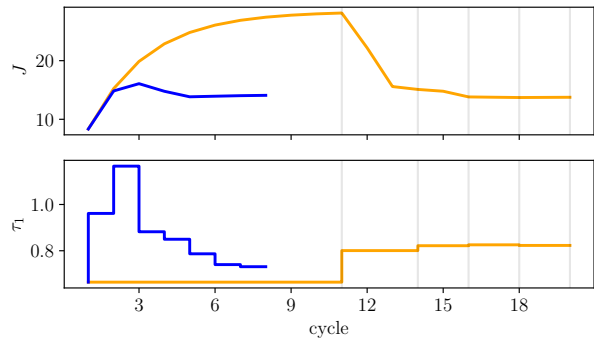


Fig. 4: Depicting the optimization of the monitoring durations  $\tau$  for the small experiment utilizing both variant (i) (yellow) and (ii) (blue). The first plot shows the cost per cycle, and the second plot shows the evolution of  $\tau_1$ . The vertical lines indicate the cycles where (i) reaches steady state.

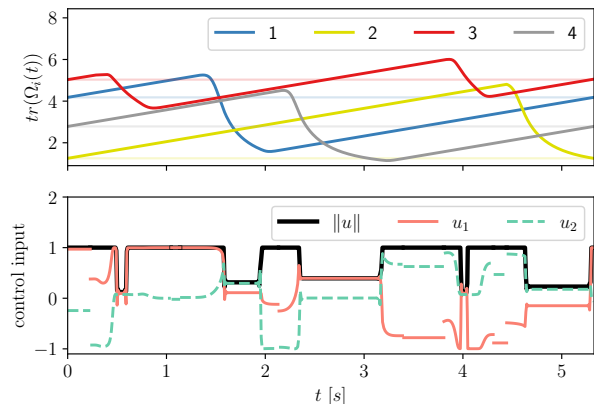


Fig. 5: Depicting the optimized steady-state control law together with the mean estimation errors.

are respected and that the mean estimation errors are indeed periodic. Both variants converge to the same cycle, which is identical to the one shown in Fig. 1.

To show that the method extends to more complex scenarios, we consider another setting with 20 regions and 10 targets. Fig. 6 again demonstrates that directly updating the configuration after each cycle reduces the number of cycles required to reach the local optimum. Finally, we note that the cost iterations, even for variant (i), are not monotonic. This is due to the fact that the step size may be too large and result in a cost increase in the current iteration. This is also reflected in the oscillation of the plotted monitoring duration. Fig. 7 shows that both variants converge to the same cycle.

## VI. CONCLUSION AND FUTURE WORK

In this paper we presented a novel PM formulation by assuming that the agent has piecewise smooth dynamics. With the goal of optimizing an average steady-state mean estimation error, we designed a periodic agent trajectory in two stages. First, in an offline approach, we created a global path planner and computed a target visiting sequence. This yielded an initial cycle for the

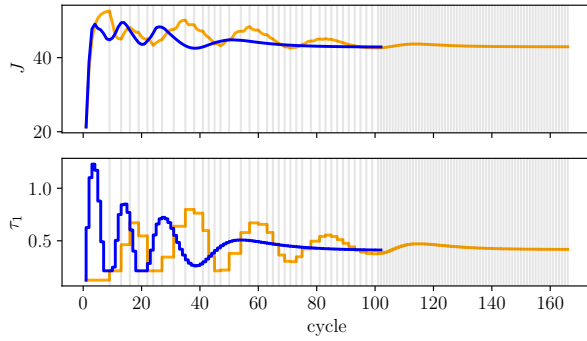


Fig. 6: Same as Fig. 4 but for the larger experiment. Vertical lines indicate times at which variant (i) updates the  $\tau_k$ .

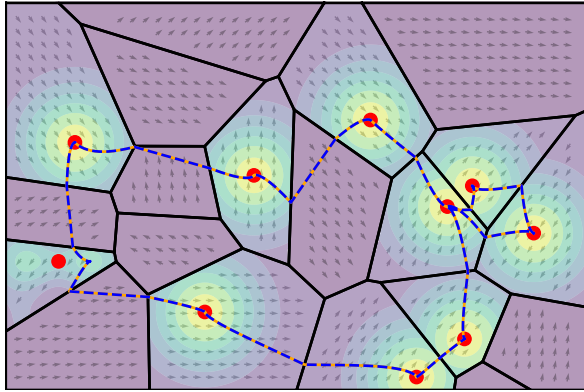


Fig. 7: The optimized configurations lead to the same cycle for both methods (i) (yellow) and (ii) (blue).

agent to follow; this cycle was then optimized online. Simulations support rapid convergence to the optimal configuration for a given visiting sequence, at least under the settings considered.

While the approach we developed is a complete solution of the PM problem defined, improvements on each level are possible. For instance, we currently do not optimize the switching segments with respect to the global cost metric – they are computed once and fixed afterwards. Their optimization in a global sense could benefit the overall performance. This is not a straightforward task, since even small alterations can change the traversed regions along the switching path. It is conceivable that suddenly another target region is visited along the altered switching path, which modifies the visiting sequence and requires the addition of a new monitoring segment.

## REFERENCES

- [1] R. N. Smith, M. Schwager, S. L. Smith, B. H. Jones, D. Rus, and G. S. Sukhatme, “Persistent ocean monitoring with underwater gliders: Adapting sampling resolution,” *Journal of Field Robotics*, vol. 28, no. 5, pp. 714–741, 2011.
- [2] D. W. Casbeer, D. B. Kingston, R. W. Beard, and T. W. McLain, “Cooperative forest fire surveillance using a team of small unmanned air vehicles,” *International Journal of Systems Science*, vol. 37, no. 6, pp. 351–360, 2006.

- [3] S. C. Pinto, N. A. Vickers, F. Sharifi, and S. B. Andersson, “Tracking multiple diffusing particles using information optimal control,” in *2021 American Control Conference (ACC)*, pp. 4033–4038, IEEE, 2021.
- [4] Y. Zhu and S. B. Andersson, “Control policy optimization for data harvesting in a wireless sensor network,” in *2022 IEEE 61st Conference on Decision and Control (CDC)*, pp. 7437–7442, IEEE, 2022.
- [5] S. K. K. Hari, S. Rathinam, S. Darbha, K. Kalyanam, S. G. Manyam, and D. Casbeer, “Optimal UAV route planning for persistent monitoring missions,” *IEEE Transactions on Robotics*, vol. 37, no. 2, pp. 550–566, 2020.
- [6] A. Nurkanović and M. Diehl, “NOSNOC: A software package for numerical optimal control of nonsmooth systems,” *IEEE Control Systems Letters*, 2022.
- [7] J. Hall, A. Nurkanovic, F. Messerer, and M. Diehl, “LCQPow: A solver for linear complementarity quadratic programs,” *arXiv preprint arXiv:2211.16341*, 2022.
- [8] S. Karaman and E. Frazzoli, “Incremental sampling-based algorithms for optimal motion planning,” *Robotics Science and Systems VI*, vol. 104, no. 2, pp. 267–274, 2010.
- [9] X. Lan and M. Schwager, “Planning periodic persistent monitoring trajectories for sensing robots in gaussian random fields,” in *2013 IEEE International Conference on Robotics and Automation*, pp. 2415–2420, IEEE, 2013.
- [10] J. Hall, L. E. Beaver, C. G. Cassandras, and S. B. Andersson, “A bilevel optimization scheme for persistent monitoring,” in *2023 62nd IEEE Conference on Decision and Control (CDC)*, pp. 247–252, 2023.
- [11] A. F. Filippov, *Differential equations with discontinuous right-hand sides: control systems*, vol. 18. Springer Science & Business Media, 2013.
- [12] J. Cortes, “Discontinuous dynamical systems,” *IEEE Control systems magazine*, vol. 28, no. 3, pp. 36–73, 2008.
- [13] X. Lan and M. Schwager, “A variational approach to trajectory planning for persistent monitoring of spatiotemporal fields,” in *2014 American Control Conference*, pp. 5627–5632, IEEE, 2014.
- [14] M. Ostertag, N. Atanasov, and T. Rosing, “Trajectory planning and optimization for minimizing uncertainty in persistent monitoring applications,” *Journal of Intelligent & Robotic Systems*, vol. 106, no. 1, pp. 1–19, 2022.
- [15] S. C. Pinto, S. B. Andersson, J. M. Hendrickx, and C. G. Cassandras, “Optimal periodic multi-agent persistent monitoring of a finite set of targets with uncertain states,” in *2020 American Control Conference (ACC)*, pp. 5207–5212, IEEE, 2020.
- [16] S. Welikala and C. G. Cassandras, “Event-driven receding horizon control for distributed persistent monitoring in network systems,” *Automatica*, vol. 127, p. 109519, 2021.
- [17] S. C. Pinto, S. B. Andersson, J. M. Hendrickx, and C. G. Cassandras, “Multi-agent persistent monitoring of targets with uncertain states,” *IEEE Transactions on Automatic Control*, 2022.
- [18] L. Zhao, W. Zhang, J. Hu, A. Abate, and C. J. Tomlin, “On the optimal solutions of the infinite-horizon linear sensor scheduling problem,” *IEEE Transactions on Automatic Control*, vol. 59, no. 10, pp. 2825–2830, 2014.
- [19] A. V. Rao, “A survey of numerical methods for optimal control,” *Advances in the Astronautical Sciences*, vol. 135, no. 1, pp. 497–528, 2009.
- [20] S. P. Boyd and L. Vandenberghe, *Convex optimization*. Cambridge university press, 2004.
- [21] J. A. Andersson, J. Gillis, G. Horn, J. B. Rawlings, and M. Diehl, “Casadi: a software framework for nonlinear optimization and optimal control,” *Mathematical Programming Computation*, vol. 11, no. 1, pp. 1–36, 2019.
- [22] A. Wächter and L. T. Biegler, “On the implementation of an interior-point filter line-search algorithm for large-scale nonlinear programming,” *Mathematical programming*, vol. 106, pp. 25–57, 2006.